In-beam spectroscopic studies of shape coexistence and collectivity in the neutron-deficient Z $\approx$ 82 nuclei

R. Julin, T. Grahn, J. Pakarinen, P. Rahkila

University of Jyvaskyla, Department of Physics, P. O. Box 35, FI-40014 University of Jyvaskyla, Finland

E-mail: rauno.julin@jyu.fi

July 2015

Abstract. In the present paper we focus on studies of shape coexistence in even-mass nuclei in the neutron-deficient Pb region. They are based on experiments carried out using tagging techniques in the Accelerator Laboratory of the University of Jyväskylä, Finland. Excited states in many of these nuclei can only be accessed via fusion-evaporation reactions employing high-intensity stable-ion beams. The key features in these experiments are high selectivity, clean spectra and instrumentation that enables high count rates. We review three spectroscopic highlights in this region.

PACS numbers: 21.10.Ky, 21.10.Re, 21.10.Tg, 23.20.Lv, 27.70.+q, 27.80.+w

Keywords: shape coexistence, nuclear reactions, in-beam γ-ray spectroscopy, measured E_γ, I_γ , $\gamma\gamma$-coinc., mean lifetimes, recoil distance Doppler-shift method, extracted $B(E2)$, quadrupole moment, deformation parameters, JUROGAM

Submitted to: *J. Phys. G: Nucl. Part. Phys.*

1. Introduction

One of the key issues in nuclear structure physics is the evolution of nuclear collectivity as a function of mass, isospin and angular momentum [1]. For example, the microscopic origin of quadrupole collectivity and shape coexistence at low excitation energies in neutron mid-shell nuclei near the $Z = 50$ and 82 shell closures are still not well understood. In some of these nuclei, deformed intruder states coexist with nearly spherical normal states [2], while in some of them intruder structures play a role in generating low-lying quadrupole vibrational states [3]. These intruder structures are usually associated with multi-proton excitations across the main shell gap.

A review of our experimental results on coexisting structures in even-mass mid-shell Cd, Sn and Te nuclei is presented in [3]. These nuclei in the $Z = 50$ region lie in the valley of stability and can be studied comprehensively via many types of reactions and beta decay. On the contrary, the neutron mid-shell $Z \approx 82$ nuclei are very neutron deficient lying close to the proton drip line and are therefore more difficult to populate in their excited states. It is important that they can be produced in fusion-evaporation reactions with stable heavy-ion beams and stable targets rendering it possible to employ a recoil separator in Recoil-Decay Tagging (RDT) measurements [4, 5, 6]. A major breakthrough was achieved when large Ge-detector arrays were combined with a high-transmission gas-filled recoil separator RITU [7] for RDT experiments in the Accelerator Laboratory of the University of Jyväskylä, Finland (JYFL). For the first time, it was shown that in-beam γ-ray spectroscopic studies of exotic α-decaying nuclei with production cross sections down to ≈ 10 nb are possible. The scientific results include first observations of excited states in around 50 isotopes of $Z = 40 - 103$. Relevant to the present article, apart from the excited 0^+ state in ^{184}Pb, all known excited states in Pb isotopes beyond the neutron $N = 104$ mid-shell have been observed only at JYFL [8, 9, 10, 11, 12]. The latter results reflect the evolution of intruder configurations in the very exotic Pb isotopes visualised in figure 1, where the level-energy systematics of the neutron-deficient Pb isotopes for $I \leq 10$ is plotted. In total, the JYFL Nuclear Spectroscopy group has dedicated around 400 days of beam on the target for the experimental programme investigating the shape coexistence in the neutron-deficient Pb region, with the vast majority of them employing the RDT technique. The advent of digital electronics has enabled performing experiments with counting rates of individual detectors as high as $\sim$30 kHz, compared to the conventional analogue limit of $\sim$10 kHz, without compromising the performance.

First results from tagging studies of neutron-deficient $Z \approx 82$ nuclei are summarized in our review article [13]. In the present paper we focus on examples illustrating more recent achievements of similar studies. The first example in section 2 shows how a high statistics RDT experiment enables to identify non-yrast states in ^{186}Pb and confirms the coexistence of different shapes by observation of collective bands built upon different minima. In section 3 we demonstrate how extremely clean γ-ray energy spectra provided by the RDT technique reveal the survival of coexisting minima even beyond the proton drip line. In the third example in section 4, systematic behaviour of collectivity of intruder bands is discussed, based on the mean lifetime measurements, where a plunger device was used in tagging experiments.

2. Non-yrast states in the mid-shell ^{186}Pb isotope through high-statistics in-beam RDT experiments

Alpha-decay studies reveal that the ground state and two first excited states in the mid-shell nucleus ^{186}Pb form a unique triplet of 0^+ states of spherical, oblate and prolate shapes, respectively [16]. The 650 keV 0^+_3 state is assumed to be the band head of a collective yrast band which, due to similarities with yrast bands in Hg and Pt isotones,

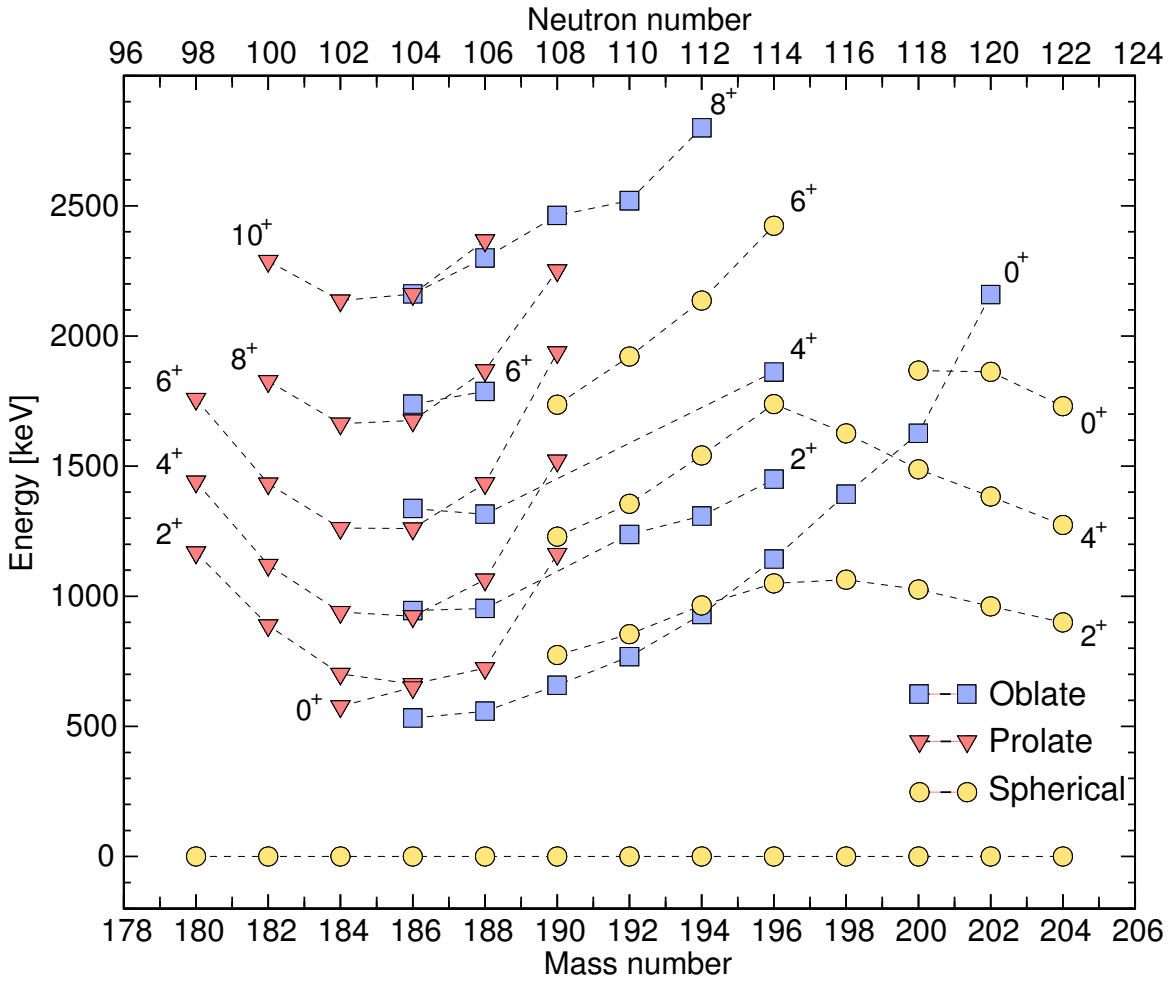

Figure 1. Level energy systematics of the neutron-deficient Pb isotopes (see [10, 14, 15] and references therein). The different intrinsic configurations have been labelled and connected with dashed line to guide the eye. The same colour-coding follows through-out the present paper.

has been assigned to a prolate shape. To verify the conclusions drawn from the α-decay studies, it is very important to observe excited states based also on the other shapes, especially a non-yrast band of oblate character. The observation of such a band should shed light on shape mixing and the evolution of shape at higher spin. Yrast bands associated with oblate intruder structures have also been observed in ^{192}Po, ^{194}Po and ^{198}Rn nuclei [13].

2.1. Upgraded RDT instrumentation

The level spacing in all the observed oblate bands is larger than that of the prolate bands. Therefore, in spite of the low energy of 532 keV of the assumed oblate 0^+ state in ^{186}Pb, the oblate band is expected to lie well above the yrast line and therefore to be weakly populated in fusion-evaporation reactions. The production cross section of

^{186}Pb in the available fusion-evaporation reactions is only on the order of 100 μb and its half-life of 4.8 s is relatively long for tagging measurements. Therefore, a new upgraded system for the RDT measurements at JYFL was needed to collect high-statistics RDT $\gamma\gamma$ coincidence data for ^{186}Pb [17]. The system comprised of the JUROGAM Ge-detector array [17] at the target area of RITU, the GREAT spectrometer [18] at its focal plane and the Total Data Readout [19] system based on time stamping. A beam of ^{83}Kr ions of 355 MeV was used to populate excited states of ^{186}Pb via the ^{106}Pd(^{83}Kr,3n)^{186}Pb reactions.

2.2. Detailed information from the high-statistic $\gamma\gamma$ coincidence data

The collected high-statistics RDT data enabled detailed $\gamma\gamma$ coincidence studies and deduction of multipolarity information from γ-ray angular distributions. Sample γ-ray energy spectra which are used to identify the prolate and oblate bands are shown in figure 2. The resulting level spectrum with four collective bands (figure 3) indicates that above its spherical ground state ^{186}Pb would behave like any deformed nucleus. The upbend seen in the prolate yrast band can be due to an alignment of $\nu(i_{13/2})^2$ or $\pi(h_{9/2})^2$. Based on systematics and similarities observed in neighbouring Os, Pt and Hg nuclei, the odd-spin states are associated as being members of octupole- and γ-vibrational bands built on the deformed prolate minimum.

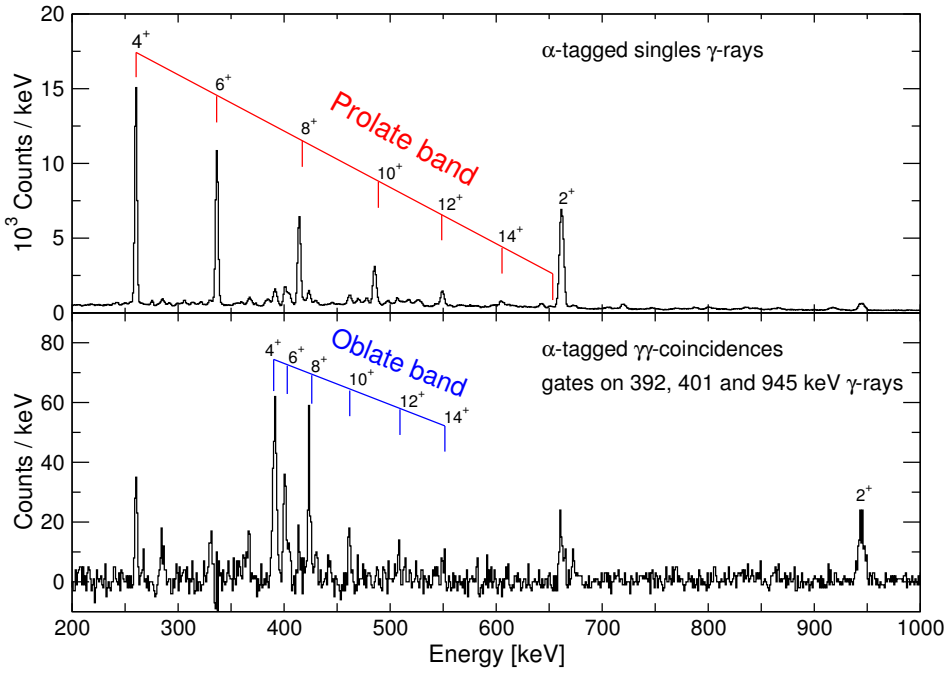

Figure 2. Gamma-ray energy spectra of the two rotational bands built upon different deformed minima in ^{186}Pb. Transitions are labelled according to spin and parity of their initial state.

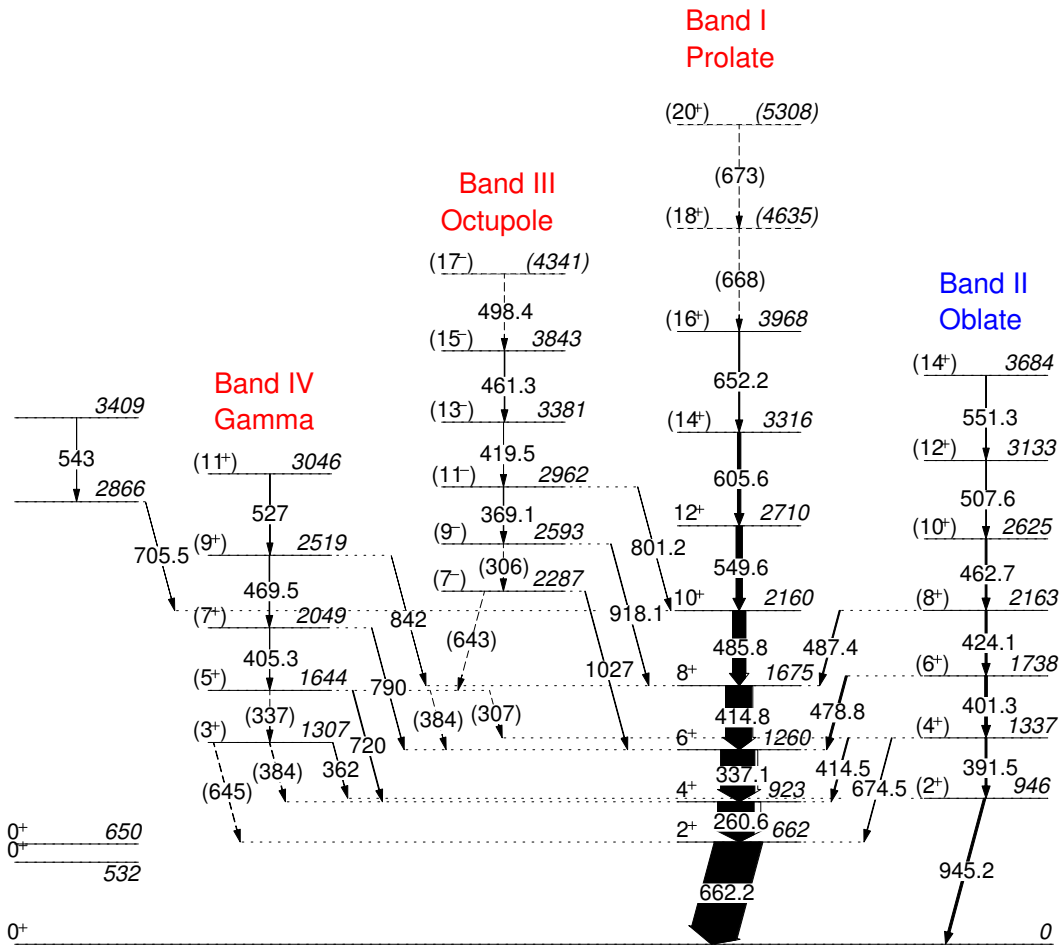

Figure 3. Level scheme of ^{186}Pb reproduced from the data of reference [14] (the two 0^+ states on the left side are taken from reference [16]). Bands have been labelled in decreasing order of their intensities and associated according to their behaviour or the predominant shape of their band-head state.

2.3. Identification of the oblate band

At first sight, without detailed examination Band II could be associated with a β-vibrational band or even-spin members of the proposed γ-vibrational band. A remarkable feature of this band are the strong $I \rightarrow I$ and weak $I \rightarrow I-2$ inter-band transitions to the prolate yrast band (Band I). For a β band based on the prolate minimum, the higher energy $E2$ ($I \rightarrow I-2$) branches to Band I should be dominant ($M1$-transitions of $\Delta I = 0$ between $K = 0$ bands are forbidden). Similar arguments make also a γ band an unlikely explanation. Instead, Band II could be built on the oblate minimum. The strong $I \rightarrow I$ inter-band transitions are then due to mixing of two different shapes.

The kinematic moments of inertia $\mathcal{J}^{(1)}$ for Band II in ^{186}Pb, together with the oblate bands in ^{182}Pt, ^{188}Pb and ^{192,194}Po, are plotted in figure 4. For comparison, the values of $\mathcal{J}^{(1)}$ for the prolate bands in ^{184,186}Pb are also shown. In general, the kinematic moments of inertia values for the prolate bands are higher than those for

the equally regular oblate bands in ^{192,194}Po. The $\mathcal{J}^{(1)}$ curve for the candidate oblate band (Band II) in ^{186}Pb differs from the curves for those bands. Similarities in the kinematic moments of inertia plots can be found between the candidate oblate bands in ^{182}Pt, ^{186}Pb, and ^{188}Pb. They extend from small $\mathcal{J}^{(1)}$ values at low spin to values that are higher than those for the oblate bands in ^{192,194}Po. One explanation would be a shape change toward a more deformed oblate structure as predicted by calculations [20, 21, 22]. Some support can also be found for the interpretation that this behaviour is due to mixing of oblate states and the unseen even-spin states of the γ band.

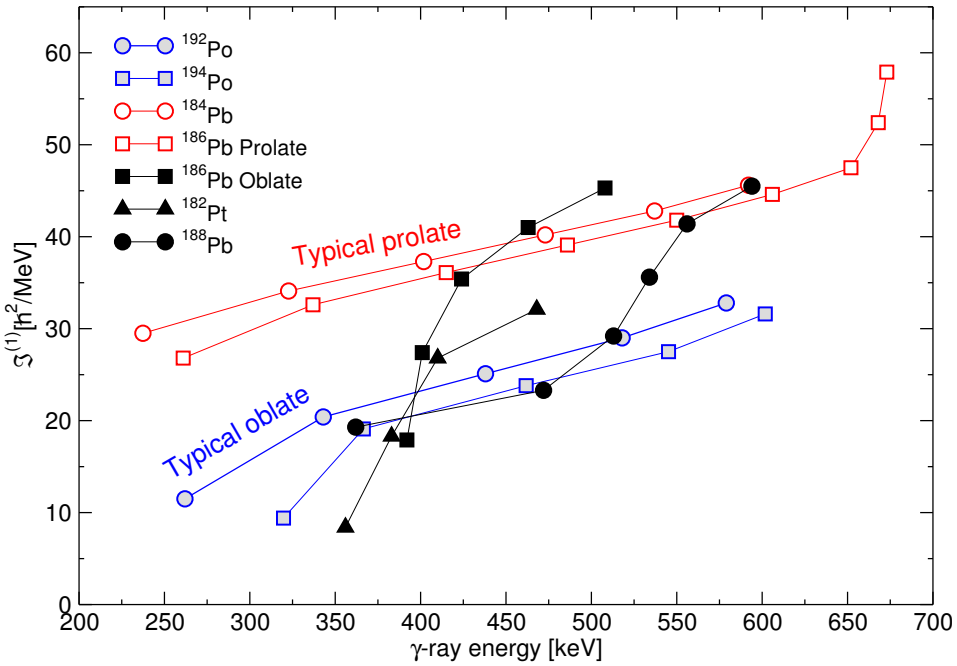

Figure 4. Kinematic moments of inertia $\mathcal{J}^{(1)}$ as a function of γ-ray energy for the two collective bands in ^{186}Pb, together with those for known bands in nuclei close to ^{186}Pb. Figure is reproduced from the data of reference [14].

2.4. The need for electron spectroscopy

For the verification of the oblate band in ^{186}Pb, it would be important to observe possible $E0$ components in the $I \rightarrow I$ transitions. Such components should occur due to the mixing between the oblate and prolate shape. As the $E0$ transitions proceed only via electron conversion, they could be seen as missing γ-ray intensities. Statistics obtained in our γ-ray measurement for ^{186}Pb is unfortunately not quite enough for such analysis. Therefore, in-beam RDT conversion-electron measurements are called for. In such measurements the existence of the two low-lying 0^+ states could also be confirmed by observing their $E0$-type de-excitation to the ground state.

3. Shape coexistence at the proton drip line

The ^{180}Pb isotope is a short-living α emitter rendering it possible to demonstrate the power of the RDT technique at the extreme of the production cross section. It represents an example, where resulting extremely clean in-beam γ-ray energy spectra of low statistics can reveal important information from isotopes at the drip line.

In-beam γ-ray studies of ^{184}Pb [8] and ^{182}Pb [9] at JYFL have revealed that the prolate intruder 4p-4h configuration minimises its energy at the $N = 104$ neutron mid-shell and its rise beyond the mid-shell is rather rapid. Moreover, beyond-mean-field calculations [21, 22, 23] extending down to $A = 182$ predict the disappearance of the oblate 2p-2h minimum in the lightest lead isotopes. Another question arises from the proximity of the proton drip-line. The isotope ^{180}Pb lies at the edge of the proton drip-line since one proton and two proton separation energies are listed as 930(50) keV and 200(25) keV, respectively [24]. Therefore, all of the excited states of ^{180}Pb are expected to be proton unbound.

3.1. Utilizing the cold reaction channels

Before our experiments performed at JYFL, very little was known about ^{180}Pb. Only its α decay with $E_\alpha = 7250(15)$ keV and $T_{1/2} = 4.5(11)$ ms has been identified [25]. For our study of ^{180}Pb an approach of utilizing symmetric reactions was taken. They provide the most favourable reaction Q-values and therefore, have excellent characteristics for a RDT measurement as the number of open evaporation channels is small and fission survivability is greatly improved relative to a typical asymmetric reaction. Consequently, the ^{90}Zr beam of 400 MeV was employed to populate excited states of ^{180}Pb via the ^{92}Mo(^{90}Zr,2n) reaction. Prompt γ rays were detected by the JUROGAMII Ge-detector array [10]. Evaporation residues were separated from the beam particles and other unwanted products by the RITU separator and were implanted into the DSSDs of the GREAT spectrometer. All detectors were instrumented using the TDR data acquisition and electronics.

3.2. In-beam spectroscopy at the level of 10 nb

The RDT analysis was complicated in the present study by the presence of a 1.5 ms α-decaying isomer in ^{179}Tl. Fortunately, both ^{176}Hg, the α-decay daughter of ^{180}Pb, and the grand-daughter, ^{172}Pt, have rather short half-lives ($\approx$20 ms and $\approx$96 ms, respectively) and large α-decay branches ($\approx$95%) in both cases, allowing the use of multi-step genetic correlations to be used to cleanly tag ^{180}Pb recoils. The value of 7254(7) keV obtained for the ^{180}Pb α-decay energy and 4.1(3) ms for the half-life are in good correspondence with recent measurements by Andreyev et al. [26]. In total, 271 full-energy recoil-α-α correlations were observed during the 160 h of irradiation with an average beam current of 7 pnA. Taking into account the RITU transmission and the detection efficiency of the α particles, the production cross section for ^{180}Pb

is estimated to be 10 nb, one of the lowest cross sections ever exploited in a successful in-beam spectroscopy experiment.

3.3. Excited states in ^{180}Pb

The singles γ-ray energy spectrum correlated with the recoil-α-α decay chains is presented in figure 5. Four γ-ray transitions with energies of 278, 312, 380, and 1168 keV are firmly assigned to ^{180}Pb. Assuming that they form a cascade, they can be ordered on the basis of their relative intensities and on the systematics. Accordingly, it is proposed that the 1168 keV γ ray, which has much higher energy than the other γ rays, corresponds to the $2^+ \rightarrow 0^+$ transition in keeping with that observed in $^{182-188}$Pb. The three further γ rays belong to a collective band above the 2^+ state. The lack of observed Pb K X-rays supports the $E2$ assignment for the three low-energy transitions. The proposed level scheme is in good agreement, in a qualitative sense, with a smooth extrapolation of the trends seen in the neighbouring even-even Pb nuclei (see figure 1 and figure 6), where the prolate-deformed states are suggested to move up in energy relative to the ground state beyond the neutron mid-shell at $N = 104$.

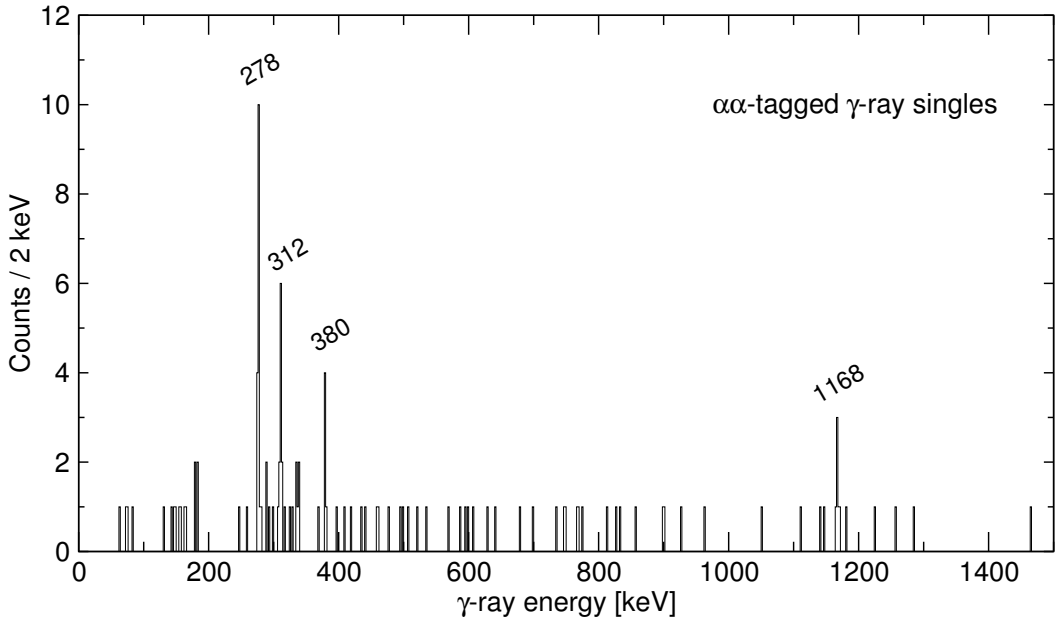

Figure 5. Recoil-gated α-α tagged γ-ray energy spectrum of ^{180}Pb. Peaks associated with the yrast band transitions have been labelled. Figure is reproduced from the data of reference [10].

3.4. Details in energy differences

Kinematic moments of inertia for transitions above the 2_1^+ state and level energy systematics lined-up with the 4_1^+ state for the even-mass $^{180-190}$Pb isotopes are shown in figure 6. At this level of detail, differences are seen between the behaviour of ^{180}Pb

and its neighbours, ^{182}Pb and ^{184}Pb. In particular, the $4^+ \rightarrow 2^+$ transition energy is almost 50 keV larger than that for ^{182}Pb, while the $6^+ \rightarrow 4^+$ transition energies are almost identical in the two nuclei. In the case of ^{182}Pb, it was concluded from a variable moment-of-inertia fit to the states above $I = 6$ that the 4^+ state is depressed slightly from its expected location by a few keV but that the 2^+ state is more strongly depressed in energy, presumably due to mixing [9]. Extending these conclusions would imply that the 2^+ state in ^{180}Pb is even more strongly depressed from its expected location. Such behaviour is also seen in the low-energy part of the prolate band in ^{188}Pb (see figure 6) where it has been attributed to strong mixing with spherical and oblate configurations coexisting at similar energies [27, 28]. While there is superficial similarity between the low-energy behaviour of the prolate band in ^{180}Pb and the one in ^{188}Pb, the origin is likely to be different because in ^{180}Pb the oblate structure is predicted to disappear or lie at much higher energy. This suggests that it may be mixing with the spherical 2^+ state, which is a more likely explanation in the case of ^{180}Pb.

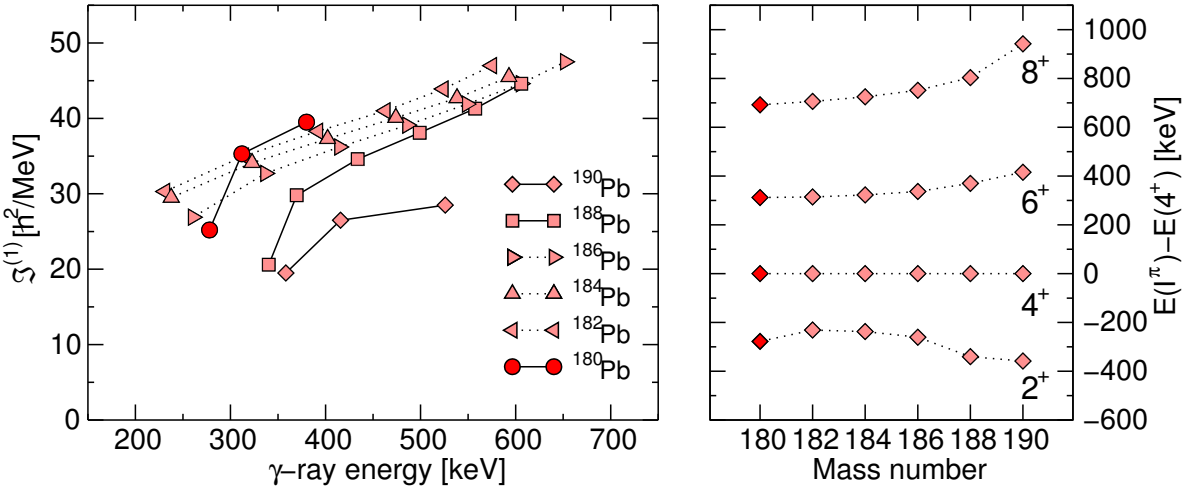

Figure 6. Properties of the rotational bands associated with the 4p-4h intruder configuration in the neutron-deficient Pb nuclei. Left: kinematic moments of inertia for transitions above the 2_1^+ state. The bands with small configuration mixing are plotted with dotted line, whereas the bands were the low-spin states are mixed are plotted with continuous line. Right: level energy systematics lined-up with the 4_1^+ state.

4. Transition rate measurements at extremes

Transition probabilities can shed light on the microscopic structures of collective excitations. Experimentally such studies are challenging not only because of extremely low production cross sections but also due to the lack of suitable measurement techniques. The direct (electronic) measurements of mean lifetimes τ are not applicable for fast decays of collective excitations possessed in nuclei in the vicinity of $N = 104$ and $Z = 82$. In addition, very exotic nuclei such as ^{186}Pb are currently beyond the reach of

Coulomb excitation studies with radioactive beams.

A variant of the Recoil Distance Doppler-Shift (RDDS) (see e.g. reference [29] and references therein) method was developed at JYFL together with University of Köln in which the RDT method was combined with the plunger device for measurements of mean lifetimes of excited states. Our first experiments with such a technique are reported in reference [28]. In those pioneering experiments a standard stopper foil of the plunger device was replaced by a degrader foil. Therefore, the nuclei of interest (recoils) produced via fusion-evaporation reactions were *not stopped* but *slowed down* in the degrader foil. This allowed the recoils to be separated by RITU and implanted at the focal-plane spectrometer GREAT, and subsequently enabled the use of the recoil-gating and RDT techniques. More detailed description of the method can be found in reference [30].

4.1. Experimental limitations and sensitivity of JUROGAM at RITU

While the RDDS method is well established, mean-lifetime measurements with the plunger device requiring recoil identification pose additional experimental difficulties and constraints. Introduction of an additional foil (degrader foil) after a reaction target increases angular straggling of the recoils and therefore decreases the transmission of RITU. In addition, the beam impinging on the degrader foil is an extra source for background γ rays which is seen in increased Ge-detector counting rates. The third implication of the degrader foil is that the energy difference between the two components (fully shifted and degraded) of a transition in a γ-ray energy spectrum is not comparable to that obtained with the standard plunger device with the stopper foil, in which the components are well separated in energy (c.f. reference [29]). Typical recoil velocities before and after the degrader foil are ≈ 0.04c and ≈ 0.03c, respectively, with a 1 mg/cm^2 Mg degrader foil used in the plunger device at RITU.

Despite the experimental challenges, we have carried out RDDS experiments in cases with the production cross section down to 120 μb (^{194}Po [28]). A key feature in the RDDS experiments utilizing RDT is virtually background-free γ-ray spectra like the one demonstrated in figure 7 in the case of ^{194}Po, for which we have measured the lifetimes of the 2^+ and 4^+ yrast states.

4.2. Collectivity around ^{186}Pb

As it was discussed earlier, kinematic moments of inertia of rotational bands can be used as an approximate measure of collectivity since they can be roughly grouped into prolate and oblate groups (see figure 4). From figure 6 one can observe that the kinematic moments of inertia are very similar for the prolate bands in this region. However, the different models predict different relations between the deformation parameter β_2 and the kinematic moment of inertia. For example, in the hydrodynamical model [31] the kinematic moment of inertia can be expressed as $\mathcal{J}^{(1)}_{hydr} = 3B\beta_2^2$ [32], where B is the mass parameter defined in reference [31]. The very different rigid rotor model [31] describes

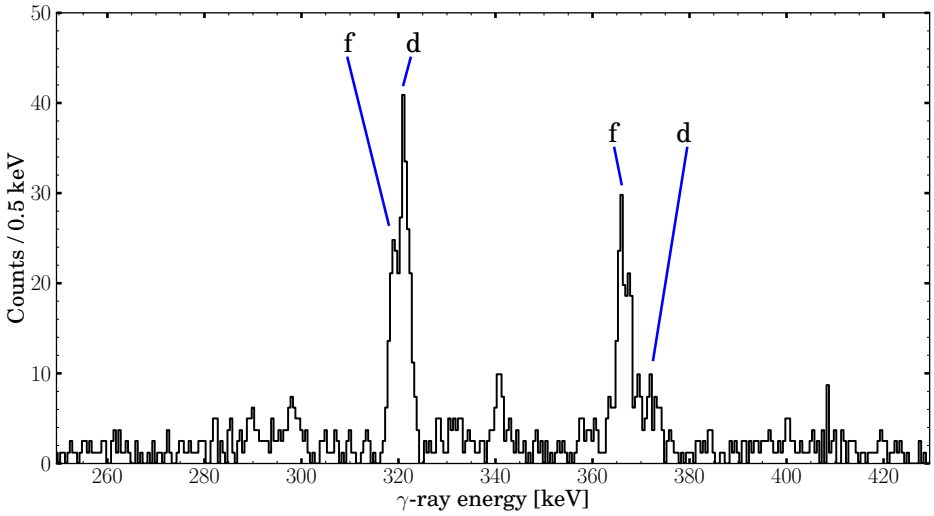

Figure 7. Recoil-gated α tagged γ-ray energy spectrum of ^{194}Po [28, 30] produced via the reaction ^{114}Cd(^{83}Kr, 3n)^{194}Po and measured with five JUROGAM detectors at 158°. The 700 μm target-to-degrader distance of the plunger device was used. The fully shifted (f) and degraded (d) components of the 320 keV $2^+ \rightarrow 0^+$ and 367 $4^+ \rightarrow 2^+$ γ-ray transitions are marked.

the moment of inertia as $\mathcal{J}^{(1)}_{rigid} = \frac{2}{5}MR^2(1 + 0.31\beta_2)$, where $R = 1.2A^{1/3}$ and M is the mass. These models should not be seen as realistic models of $\mathcal{J}^{(1)}$, however they can be considered as two extremes with experimental values lying somewhere in between. It is clear though that the dependence of $\mathcal{J}^{(1)}$ in the powers of β_2 varies greatly and therefore it is difficult to measure deformation from $\mathcal{J}^{(1)}$ alone.

The reduced transition probabilities, $B(E2)$ values for the $E2$-type transitions, are model independent and can be extracted from mean-lifetime measurements. In principle, one can extract information of matrix elements associated with a transition under study. We have carried out series of such measurements in Hg [33, 34], Pb [28] and Po [28, 35] around $N = 104$ with a view on the evolution of collectivity as a function of the initial angular momentum I_i and the atomic number (charge) Z.

4.3. Collectivity through rotation

In a nucleus that generates collectivity purely through the rotation, the transitional quadrupole moment Q_t is constant for the states that have the same intrinsic structure [31]. In general, the Q_t value can also be seen as a parameter used for systematic comparisons acting as a measure of collectivity. Note that one can not extract the sign of Q_t from the mean-lifetime measurements since $\tau \propto Q_t^{-2}$. In figure 8, a selection of absolute values of Q_t extracted from the mean-lifetime measurements are shown as a function of their initial spin I_i. Two features of the plot are imminent, firstly the constant values of $|Q_t|$ within the error bars for the prolate states with $I \geq 4$ in ^{186}Pb and ^{182}Hg, and the significantly lower but again constant $|Q_t|$ values the oblate states in

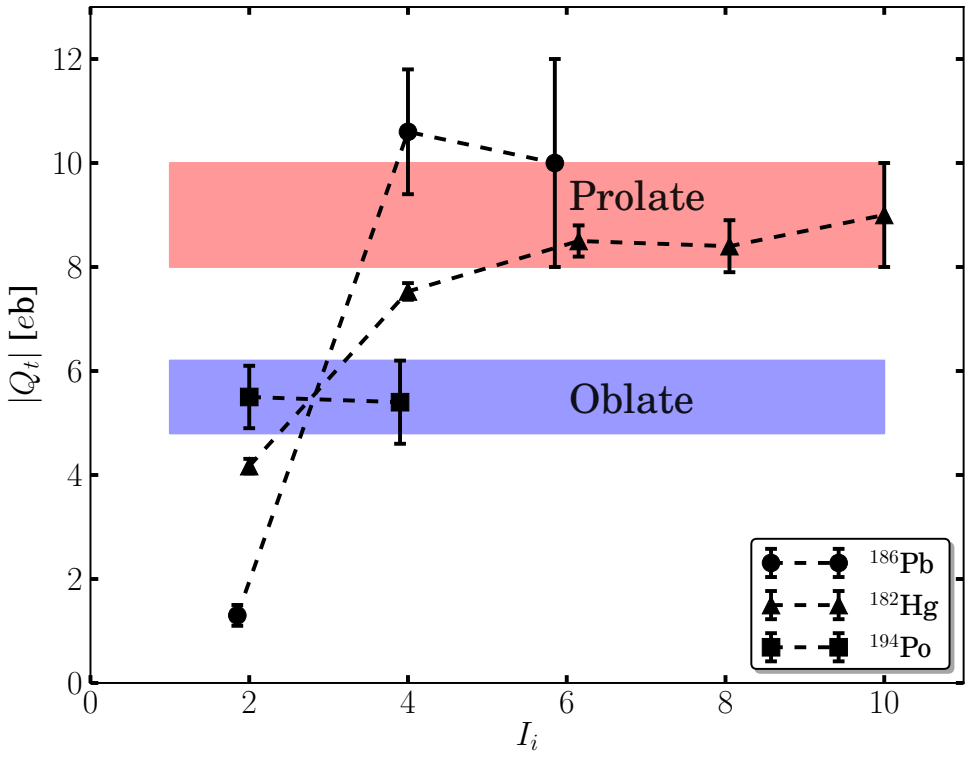

Figure 8. Transition quadrupole moment $|Q_t|$ values in ^{182}Hg [33], ^{186}Pb [28] and ^{194}Po [28] plotted as a function of the initial spin I_i. The coloured bands show the average error bars for the pure prolate and oblate configurations.

^{194}Po. Thus, figure 8 represents a direct evidence of the level of collectivity of the two coexisting configurations with very different deformations near $N = 104$ in the neutron-deficient Pb region. Another notable feature is the sudden drop in $|Q_t|$ below $I = 4$ in ^{186}Pb and ^{182}Hg. This could be explained by the remarkably different configurations for the ground states than those for the 2^+ states, pushing the $|Q_t|$ value for the $I = 2$ transitions down.

If we adopt the view of reference [36], which states that apart from the ground states of nuclei with closed shell(s), the nuclei tend to deform, the high $|Q_t|$ values of figure 8 appear to be obvious. Apart from the $2^+ \rightarrow 0^+$ transition that connects the intruder 2^+ state to the spherical ground state in the semi-magic ^{186}Pb, the collectivity is rather high. This is also the case in other nuclei in the vicinity. In general, the spherical states can be found as the ground states of the Pb nuclei and, indeed, deformation dominates the nuclear shapes of the yrast states in the neutron-deficient Pb region.

The near-constant values of $|Q_t|$ for the pure rotational states have also been measured in other neighbouring isotopes [30, 33, 35]. Since the $|Q_t|$ values are connected to the deformation parameter β_2 by the rigid rotor model [31], this demonstration of collectivity with high $|Q_t|$ values is a feature of deformation in this region of the nuclear

chart. Indeed, the constant $|Q_t|$ values, as predicted by the theory, indicate the same intrinsic structure of these states. It is remarkable to note one-to-one correspondence between the excited states assigned as prolate or oblate in figure 8 and the ones in figure 4 based on the kinematic moments of inertia.

4.4. The Z-dependence of collectivity—or the lack thereof

Since systematic mean-lifetime data have emerged, it is interesting to survey the collectivity as a function of Z along the $N = 104$ line. However, the electric quadrupole moment is by definition a function of the electric charge and therefore of Z. It is necessary to take this into account when comparing the $|Q_t|$ values of nuclei with different Z. In figure 9 the measured $|Q_t|$ values normalized by Z at or near the $N = 104$ line have been plotted as a function of Z. As we discussed above, similar $\mathcal{J}^{(1)}$ have been observed for these states suggesting similarity in their structure.

From figure 9 it is astonishing to note that for the prolate states there could be an increasing trend of collectivity as a function of Z. This behaviour is in disagreement with the assumption of the similar collectivity for these transitions deduced from $\mathcal{J}^{(1)}$. Also for the oblate states a very modest increase in collectivity can be seen.

In reference [36] the concept of "multishells" was introduced, in which several open shells are viewed as one larger shell region. For instance, when "suppressing" the $Z = 82$ closed shell line, the nucleus ^{186}Pb is at the centre of the multishells formed by the two proton and one neutron shells (see figure 48 in reference [36]). Following this idea, the neutron-deficient Pb region is at the centre of the two multishells (proton and neutron) and thus has an extremely large valence particle space. Apart from the ground states of the Pb nuclei, states of these nuclei are deformed. The collectivity should then increase when approaching the maximum valence space which in this case is in ^{186}Pb. This concept could provide an explanation for the increase of collectivity towards $Z = 82$ that is observed in figure 9. It would therefore be interesting to measure transition probabilities of the prolate states in nuclei with $Z > 82$. In the multishell concept $|Q_t|/Z$ for such states should then decrease as a function of Z. It may be premature to make any firm conclusions with the present data alone and therefore more systematic studies are required.

5. Summary and future challenges

Experiments performed at JYFL have shown that structures of nuclei close to the proton drip line can still be studied by using stable-ion beams and stable targets. This is enabled by employing fusion-evaporation reactions and the RDT technique providing extremely high selectivity and clean spectra. In the present paper we demonstrate the power of such measurements by reviewing three distinct experimental topics of the shape coexistence in the neutron-deficient Pb region. In the first one, in addition to the prolate yrast band in ^{186}Pb, high-statistics RDT data result in candidates for γ- as well

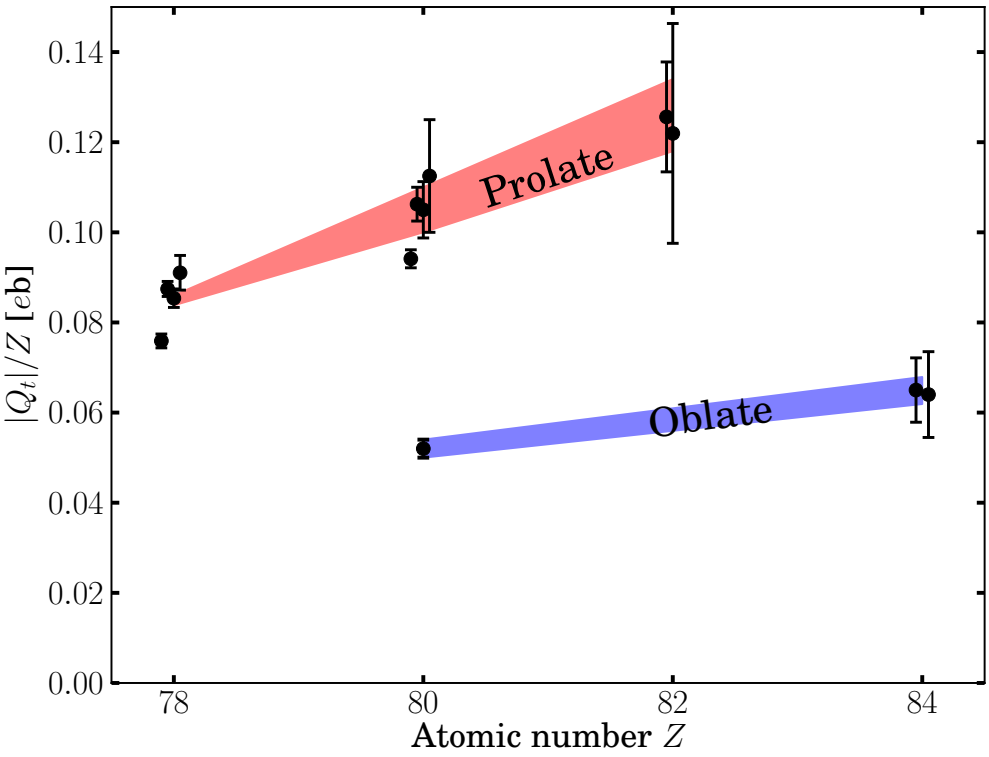

Figure 9. The measured transition quadrupole moments Q_t divided by Z as a function of Z in the ^{184}Pt [37], ^{182}Hg ($I \geq 4$) [33], ^{186}Pb ($I \geq 4$) [28] and ^{194}Po [28] nuclei for the proposed deformed states. The filled polygons illustrate the error-weighted mean values of $|Q_t/Z|$ for the prolate and oblate states.

as octupole- vibrational bands and a band with features, which indicate that it is based on the coexisting oblate minimum. The second topic represents a case at the extreme of nuclear spectroscopy: the ^{180}Pb isotope was populated via a cold fusion-evaporation reaction with a cross-section of only 10 nb and still extremely clean RDT γ-ray spectra enabled to construct a level scheme revealing an interesting behaviour of its prolate yrast band. In the third topic, tagging techniques are applied to plunger mean-lifetime measurements of the intruder bands near the neutron $N = 104$ mid-shell. The results reveal the high quadrupole collectivity of the prolate bands. They also indicate that collectivity of these bands increase with increasing Z.

Since 1996, large body of data have been gathered in various types of tagging experiments at JYFL on the shape coexistence in neutron-deficient heavy nuclei. Nowadays they include comprehensive sets of in-beam and focal-plane spectroscopic studies of even- and odd-mass isotopes of elements spanning from Os to Fr. They can be combined with recent results from Coulomb-excitation experiments and measurements of nuclear radii carried out with radioactive heavy-ion beams at CERN-ISOLDE. The resulting picture is getting complete, but still many open questions remain. In the

following we list a few key topics and future experimental challenges:

- How does the oblate minimum develop beyond the neutron mid-shell? Probing of the minimum requires studies of non-yrast states through in-beam γ-ray spectroscopy.
- What is the configuration of the low-lying 2^+ states? The microscopic structure is still unknown. Systematic studies through both the safe and relativistic Coulomb excitation and transfer reactions are required.
- What is the nature of the non-yrast structures in Pb isotopes around mid-shell (i.e. rotational oblate or β vibration, also in a bigger picture; do we have β vibrators). Monopole strengths from the recoil shadow conversion electron spectroscopy are required.
- Confirmation of the three different shapes in a single nucleus is still missing. Complementary studies through combination of all techniques can pinpoint this.
- Apart from transfer reactions, what else could we learn from experiments employing storage-ring experiments such as EXL at ESR [38] in future facilities? Angular momentum transfer in proton (neutron) knock-out reaction through momentum distribution measurement at focal planes of fragment separators may reveal proton (neutron) contributions.

Acknowledgements

This work has been supported by the Academy of Finland under the Finnish Centre of Excellence Programme 2006-2011 and 2012-2017 (Nuclear and Accelerator Based Physics Programme at JYFL) and by the I3 projects EURONS and ENSAR of the EU 6th and 7th Framework Programmes. The GAMMAPOOL European Spectroscopy Resource is greatly acknowledged for the loan of germanium detectors for JUROGAM.

References

[1] *Perspectives of nuclear physics in Europe - NuPECC long range plan* (www.nupecc.org) 2010
[2] Wood J L, Heyde K, Nazarewicz W, Huyse M and Van Duppen P 1992 *Phys. Rep.* **215** 101
[3] Julin R 1994 *Phys. Scr.* **T 56** 151
[4] Schmidt K-H *et al.* 1986 *Phys. Lett. B* **168** 39
[5] Simon S *et al.* 1986 *Z. Phys. A* **325** 197
[6] Paul E S *et al.* 1995 *Phys. Rev. C* **51** 78
[7] Leino M *et al.* 1995 *Nucl. Instrum. Methods B* **99** 653
[8] Cocks J F C *et al.* 1998 *Eur. Phys. J A* **3** 17
[9] Jenkins D G *et al.* 2000 *Phys. Rev. C* **62** 021302
[10] Rahkila P *et al.* 2010 *Phys. Rev. C* **82** 011303(R)
[11] Pakarinen J *et al.* 2009 *Phys. Rev. C* **80** 031303(R)
[12] Pakarinen J *et al.* In-beam γ-ray spectroscopy of ^{183}Pb, to be published
[13] Julin R, Helariutta K and Muikku M 2001 *J. Phys. G: Nucl. Part. Phys.* **27** R109
[14] Pakarinen J *et al.* 2007 *Phys. Rev. C* **75** 014302

[15] Pakarinen J *et al.* 2013 EXON-2012 Proceedings of the International Symposium Vladivostok, Russia p. 285
[16] Andreyev A N *et al.* 2000 *Nature* **405** 430
[17] Pakarinen J *et al.* 2005 *Phys. Rev. C* **72** 011304(R)
[18] Page R D *et al.* 2003 *Nucl. Instrum. Methods B* **204** 634
[19] Lazarus I H *et al.* 2001 *IEEE Trans. Nucl. Sci.* **48** 567
[20] Dracoulis G D *et al.* 2003 *Phys. Rev. C* **67** 051301
[21] Bender M, Bonche P, Duguet T and Heenen P-H 2004 *Phys. Rev. C* **69** 064303
[22] Rodríguez-Guzmán R R, Egido J L and Robledo L M 2004 *Phys. Rev. C* **69** 054319
[23] Nazarewicz W 1993 *Phys. Lett. B* **305** 195
[24] Audi G, Wapstra H and Thibault C, 2003 *Nucl. Phys. A* **729** 337
[25] Toth K S *et al.* 1999 *Phys. Rev. C* **60** 011302
[26] Andreyev A *et al.* 2009 *Phys. Rev. C* **80** 054322
[27] Dracoulis G D, Byrne A P and Baxter A M 1998 *Phys. Lett. B* **432** 37
[28] Grahn T *et al.* 2006 *Phys. Rev. Lett.* **97** 062501
[29] Dewald A, Möller O and Petkov P 2012 *Progress in Particle and Nuclear Physics* **67** 786
[30] Grahn T *et al.* 2008 *Nucl. Phys. A* **801** 83
[31] Bohr A and Mottelson B R *Nuclear Structure Volume II: Nuclear Deformations* (Singapore: World Scientific Publishing Co. Pte. Ltd.) p. 75
[32] Gupta R K 1972 *Phys. Rev. C* **6** 426
[33] Grahn T *et al.* 2009 *Phys. Rev. C* **80** 014324
[34] Gaffney L P *et al.* 2014 *Phys. Rev. C* **89** 024307
[35] Grahn T *et al.* 2009 *Phys. Rev. C* **80** 014323
[36] Heyde K and Wood J L 2011 *Rev. Mod. Phys.* **83** 1467
[37] Garg U *et al.* 1986 *Phys. Lett. B* **180** 319
[38] Egelhof P, Kisselev O, Münzenberg G, Neumaier S R and Weick H 2003 *Phys. Scr.* **T 104** 151